Collisions in Primordial Star Clusters

Formation Pathway for intermediate mass black holes

B. Reinoso[1], D.R.G. Schleicher[1], M. Fellhauer[1], R.S. Klessen[2,3], and T. C. N. Boekholt[4]

[1] Departamento de Astronomía, Facultad Ciencias Físicas y Matemáticas, Universidad de Concepción, Av. Esteban Iturra s/n Barrio Universitario, Casilla 160-C, Concepción, Chile;
e-mail: `breinoso@udec.cl`

[2] Universität Heidelberg, Zentrum für Astronomie, Institut für Theoretische Astrophysik, Albert-Ueberle-Str. 2, 69120 Heidelberg, Germany

[3] Universität Heidelberg, Interdisziplinäres Zentrum für Wissenschaftliches Rechnen, Im Neuenheimer Feld 205, 69120 Heidelberg, Germany

[4] CIDMA, Departamento de Física, Universidade de Aveiro, Campus de Santiago, 3810-193 Aveiro, Portugal

ABSTRACT

Collisions were suggested to potentially play a role in the formation of massive stars in present day clusters, and have likely been relevant during the formation of massive stars and intermediate mass black holes within the first star clusters. In the early Universe, the first stellar clusters were particularly dense, as fragmentation typically only occurred at densities above 10^9 cm^{-3}, and the radii of the protostars were enhanced due to the larger accretion rates, suggesting a potentially more relevant role of stellar collisions. We present here a detailed parameter study to assess how the number of collisions as well as the mass growth of the most massive object depends on the properties of the cluster, and we characterize the time evolution with three effective parameters, the time when most collisions occur, the duration of the collisions period, as well as the normalization required to obtain the total number of collisions. We apply our results to typical Population III (Pop. III) clusters of about 1000 $M_\odot$, finding that a moderate enhancement of the mass of the most massive star by a factor of a few can be expected. For more massive Pop. III clusters as expected in the first atomic cooling halos, we expect a more significant enhancement by a factor of $15 - 32$. We therefore conclude that collisions in massive Pop. III clusters were likely relevant to form the first intermediate mass black holes.

1. Introduction

Collisions are often considered to be important during the formation of particularly massive stars, as suggested by Bonnell et al. (1998) and Clarke & Bonnell (2008). While the formation of low- and intermediate mass stars can be readily explained through accretion and infall in a protostellar core (Bodenheimer & Sweigart 1968; Larson 1969; Shu 1977, see discussion by Palla & Stahler (1993)), 1D models originally failed for stars more massive than 20 $M_\odot$, which start core hydrogen burning while still accreting, thereby preventing further accretion through ionizing radiation (Yorke & Sonnhalter 2002). More recent work shows however that in 3D situations, there are always channels through which accretion still occurs, thus not necesarrily providing a limiting factor (Keto & Klaassen 2008; Krumholz et al. 2009; Peters et al. 2010a,b, 2011). A quantitative assessment of the role of collisions in present-day protostellar star clusters has been pursued by Baumgardt & Klessen (2011), finding that between $0.1-1\%$ of the protostars participate in such collisions within typical clusters, potentially providing a relevant enhancement for sufficiently large numbers of stars. Similar investigations have been pursued by Moeckel & Clarke (2011), Oh & Kroupa (2012a) and Fujii & Portegies Zwart (2013).

In the early Universe, the conditions are potentially even more favorable for the formation of massive objects via collisional processes. In the primordial gas, the cooling is less efficient and predominantly driven by small fractions of molecular hydrogen (see e.g. Omukai et al. 2005). As shown via numerical simulations, the typical densities where fragmentation occurs are of the order 10^9 cm^{-3} or higher (e.g. Clark et al. 2011b,a; Greif et al. 2011, 2012; Smith et al. 2011, 2012; Latif et al. 2013b), leading to the formation of dense clusters with radii of 0.1 pc or even smaller. Trace amounts of dust grains may even trigger fragmentation at still higher densities (e.g. Schneider et al. 2003, 2006; Omukai et al. 2008; Schneider et al. 2012; Klessen et al. 2012; Dopcke et al. 2011, 2013; Bovino et al. 2016; Latif et al. 2016), providing ideal conditions for the formation of very dense clusters.

In addition to the compactness of the cluster, the protostellar radii are also enhanced by the more rapid accretion expected in primordial or low-metallicity gas, thereby increasing the overall cross section for collisions. Large protostellar radii of up to 300 $R_\odot$ were calculated in stellar evolution models by Stahler et al. (1986) or Omukai & Palla (2001, 2003). It has been shown that variable protostellar accretion rates can enhance them further (Smith et al. 2012). A strong increase of the radii also seems possible in the presence of particularly high accretion rates of ~ 0.1 $M_\odot$ yr^{-1} (Hosokawa et al. 2012, 2013; Schleicher et al. 2013; Haemmerlé et al. 2017; Woods et al. 2017), implying ~ 500 $R_\odot$ for a 10 $M_\odot$ star and potentially more than 1000 $R_\odot$ for a 100 $M_\odot$ star.

It is thus conceivable that collisions may play some role in typical Population III (Pop. III) clusters as expected to form in so-called minihalos with about 10^6 $M_\odot$, as well as in the more massive atomic cooling halos with masses of the order 10^8 $M_\odot$. These more massive halos are frequently considered as the birth places of intermediate mass black hole seeds. Collisional processes were indeed mentioned as an important pathway in the

seminal paper by Rees (1984), and subsequently taken into account for instance in semi-analytical models by Devecchi et al. (2010, 2012), and Lupi et al. (2014). In N-body simulations employing cosmological initial conditions, Katz et al. (2015) and Sakurai et al. (2017) have shown that black holes with masses of $\sim 10^3$ M$_\odot$ can be formed.

Here, we present a systematic investigation on how the formation of very massive objects depends on the properties of the cluster. Our numerical setup and the initial conditions are described in section 2, and our results are described in section 3, including the time evolution of a typical cluster, the number of collisions and mass of the resulting object found under different conditions, as well as the time required to achieve such an enhancement. In section 4, the results are applied to primordial clusters, both in the context of minihalos and the larger atomic cooling halos. A final summary and discussion is given in section 5.

2. Simulation setup

We present a set of *N*-body simulations of stellar collisions in compact star clusters. We have not included the effect of a gaseous potential or modeled the effect of the gas in explicit terms. To zero order, if the latter is dominating the potential, it will primarily increase the velocity dispersion and thereby decrease the crossing time of the cluster, allowing for a larger number of crossing times in a given physical time. In addition, there can be other gas-related effects that may enhance the number of collisions, which we will discuss in section 3.5. The calculations here thus provide a conservative lower limit on the number of collisions. To perform the calculations we use a modified version of NBODY6[1] (Aarseth 2000) to treat collisions, where we switch off the stellar evolution package and instead explicitly specify the stellar radii to perform a parameter study. NBODY6 is a fourth order Hermite integrator which includes a spatial hierarchy to speed up the calculations: the Ahmad-Cohen scheme (Ahmad & Cohen 1973). It also includes routines to treat tidal circularization which is believed to be the main mechanism from which binaries are formed in star clusters. Another important routine included is the Kustaanheimo-Stiefel regularization (Kustaanheimo & Stiefel 1965), an algorithm to treat binaries and close two body encounters more accurately and faster.

2.1. The star clusters

We investigate how the number of collisions and the mass of the final object depends on the number of stars *N* and the radii of the stars R$_{star}$. We model a compact cluster in virial equilibrium consisting of equal mass stars with a total stellar mass of M$_{cluster}$ = 10^4 M$_\odot$ using a Plummer distribution for the stars (Plummer 1911) with a Plummer radius of R$_{pl}$ = 0.077 pc, implying a half-mass radius of R$_h$ = 0.1 pc. With this configuration the crossing time of the cluster is 0.022 Myr. We vary the number of stars $N = 100, 500, 1000, 5000$ and keep the mass of the cluster constant, therefore the initial masses of the stars M$_{ini}$ depend on *N* as M$_{ini}$ = M$_{cluster}$/*N*. For a fixed number of stars *N* we vary the stellar radii R$_{star}$ = $20, 50, 100, 200, 500, 1000, 5000$ R$_\odot$.

2.2. Stellar collisions

The standard version of NBODY6 includes a routine to treat stellar collisions and can be used only when the stellar evolution option is activated. The stellar evolution package included in the code is useful for metallicities ranging from Z=0.0001 up to Z=0.03 (Hurley et al. 2000). In this investigation, we are primarily interested in the application to extremely metal poor conditions, with metallicities $Z \leq 10^{-6}$. Instead of pursuing detailed stellar evolution calculations, our goal here is to determine the regime where the collisions are potentially relevant. To treat the collisions, we therefore switch off the stellar evolution routine in NBODY6, and model the collisions as follows:

A collision occurs when the separation *d* between two stars is smaller than the sum of the radii of the stars ($d \leq R_1 + R_2$). When this condition is satisfied, we replace the two colliding stars by a new one, and the mass of the new star M$_{new}$ is simply the sum of the masses of the two colliding stars M$_{new}$ = M$_1$+M$_2$. The radius of the new star R$_{new}$ is calculated with Eq. 1 using the condition that the new star should have the same density as the colliding stars:

$$R_{new} = R_1 \left(\frac{M_1 + M_2}{M_1} \right)^{1/3}. \tag{1}$$

Effectively, this assumes that the collision product quickly settles into a new equilibrium configuration in which the density corresponds to that of an unperturbed star of the same mass. This is consistent with detailed stellar evolution calculations, e.g., by Hosokawa et al. (2012) or Haemmerlé et al. (2016). Nevertheless, we emphasize that we do not aim here to follow the detailed stellar evolution.

3. Results

In the following, we describe the main results of our calculations. This includes the description of the time evolution in a typical cluster, the number of collisions that occur for different cluster parameters assuming a sufficient time of integration, a description of the time evolution and its parametrization, a discussion of ejections as well as a discussion on uncertainties and neglected processes.

3.1. Time evolution in a typical cluster

The time evolution in two typical clusters is shown in Figures 1 and 2, the first one showing a cluster with 1000 stars, and each of them having a radius of 500 R$_\odot$. The second one is a cluster with 5000 stars and each of them having the same stellar radius (500 R$_\odot$). For both clusters, we show the fraction of stellar collisions (relative to the total initial number of stars), the logarithm of the Lagrangian radii corresponding to 10%, 50% and 90% of the mass, as well as the mass of the most massive object normalized through the initial mass of the stars.

In Fig. 1, the maximum of collisions occurs clearly between 30-50 crossing times, where also the Lagrangian radius corresponding to 10% of the enclosed mass drops considerably, revealing that a massive central object has already accreted 10% of the mass at this time. Most of the collisions occur within the half mass radius of the cluster and more massive stars are formed very close to the center of the cluster where they collide to form a single very massive object. The peak fraction of collisions reaches about 1%, and the mass of the central object increases by a corresponding factor of about 100, due to a similar number of stellar collisions. The 50% and 90% Lagrangian
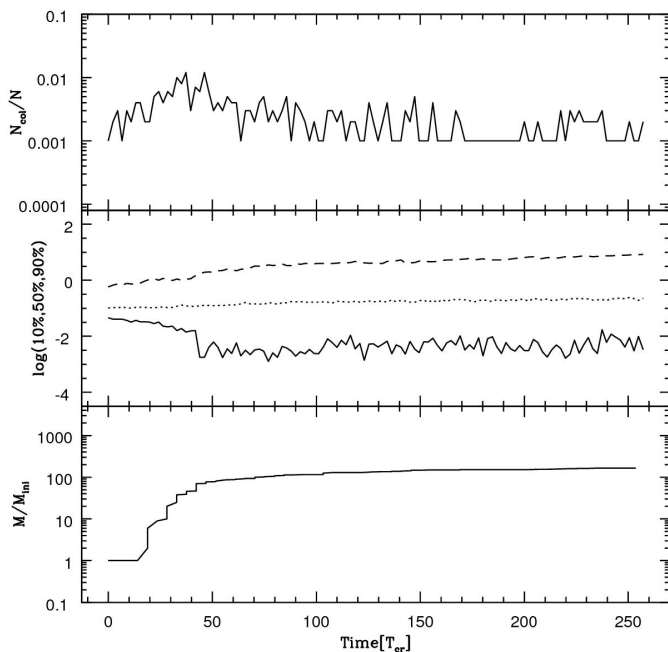
Fig. 1. Time evolution of a cluster with $N = 1000$ stars, each of them with an initial radii of $R_{star} = 500$ $R_{\odot}$. Top panel: Number of collisions divided by number of stars as a function of time. Mid panel: Logarithm of the Lagrangian radii corresponding to 10%, 50% and 90% of the enclosed mass as a function of time. Bottom panel: Mass of the most massive object divided by the initial stellar mass as a function of time. In all panels, the time is normalized by the cluster's crossing time.
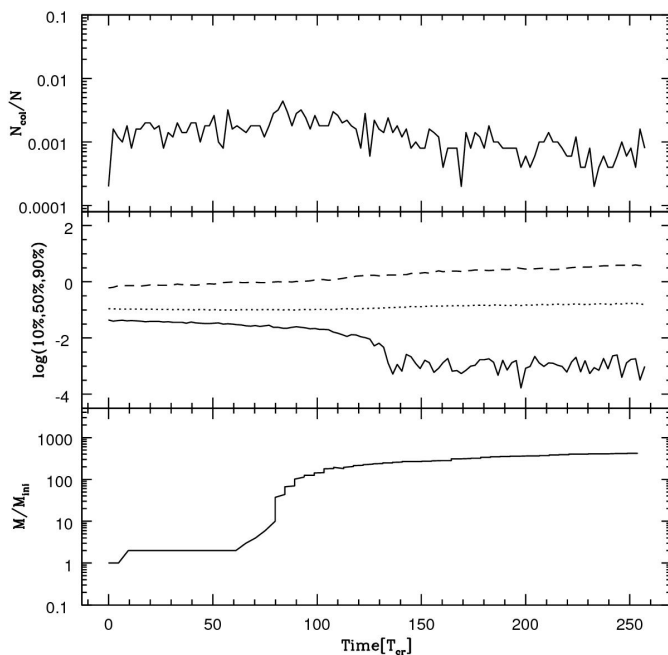

Fig. 2. Time evolution of a cluster with $N = 5000$ stars, each of them with an initial radii of $R_{star} = 500$ $R_{\odot}$. Same panels as in Fig. 1.

radius shows sings of expansion, as the cluster dissolves due to ejections.

The behavior in Fig. 2 is quite similar. The main difference is that the time over which the collisions occur is more spread out, ranging from 10 up to $130 - 150$ crossing times. While the fraction of collisions is approximately constant during that period, with values around 0.1%, the run-away growth of the most mas-

N	B	C	D	E
100	0.45 ±0.02	-2.25 ±0.06	0.40±0.04	-0.16±0.09
500	0.49 ±0.02	-2.27 ±0.06	0.53±0.04	0.22±0.09
1000	0.51 ±0.04	-2.29 ±0.09	0.57±0.06	0.44±0.14
5000	0.50±0.03	-2.16 ±0.07	0.52±0.05	1.28±0.12

Table 1. Parameters from the fit to the functions Eq. 2 (Column 2 & 3) and Eq. 3 (Column 4 & 5) to estimate the total fraction of collisions in a cluster depending on the initial radii of the stars R_{star} and the initial number N of stars (Eq. 2). Parameters D & E are used to estimate the mass of the most massive object divided by it's initial mass (M_{max}/M_{ini})at the end of the runaway growth depending on the initial radii R_{star} of the stars and the initial number N of stars (Eq. 3).

sive object begins at around 80 crossing times, suggesting that before that stage, several more massive stars had formed which subsequently merge. Once the mass of the most massive object has increased by about a factor of 500, thus corresponding to about 10% of the total mass, the corresponding Lagrangian radius decreases as seen in Fig. 1. The overall evolution in both cases is thus quite similar.

3.2. Number of collisions for different cluster parameters

Our central goal is to determine how the number of collisions and the growth of the most massive object depends on the properties of the cluster. For this purpose, we will initially assume that enough time is available until all collisions have occured, while investigating more details of the time evolution in the next subsection.
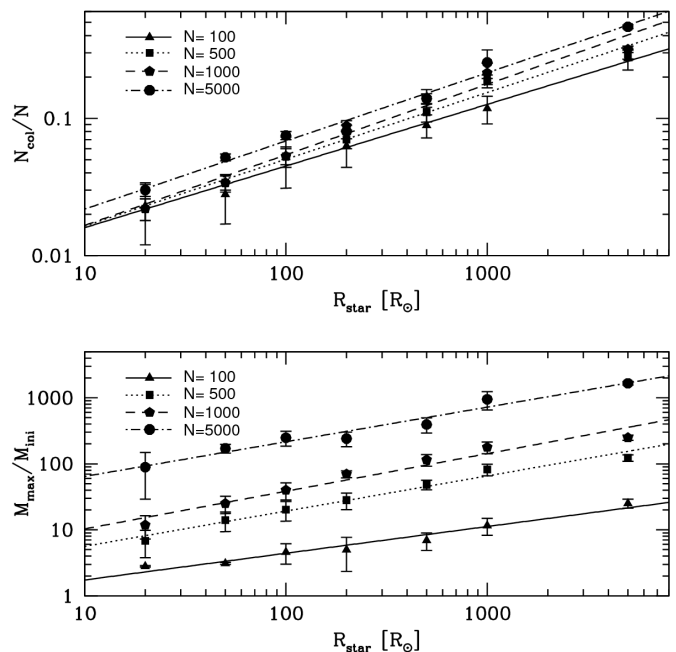

Fig. 3. Top Panel: Fraction of collisions (N_{col}/N) as function of the initial stellar radius and the number of stars, we also show the best linear fits from Eq. 2 and the parameters for these fits in Table 1. Bottom Panel: Final mass over the initial mass (M_{max}/M_{ini}) for the most massive star at the end of the runaway growth as function of the initial stellar radius and the initial number of stars. We also show the best linear fits from Eq. 3 and the parameters for these fits in Table 1.

Our main results are given in Fig. 3, showing the fraction of collisions as a function of stellar radius and for different numbers of stars. The data shown here correspond to an average over 10 simulations for each individual configuration, to improve the statistical reliability of the results. We find that the total fraction of collisions depends very weakly on the number of stars, showing an increase by at most a factor of 2 when going from 100 to 5000 stars. This very minor increase may result from the fact that a larger (but still small) fraction of the effective area is filled with stars. We do in principle not expect this to depend strongly on the IMF, but it remains one of the uncertainties to be explored in future studies. The dependence on the stellar radii on the other hand is very clear and corresponds to a power-law with slope of about 0.5 (see second column in Table 1).

The mass of the most massive object normalized by the initial mass of the stars shows a clearer dependence both on number of stars and on radius. This can be understood from the fact that the fraction of collisions is roughly independent of the number of stars. If most collisions occur with the most massive object (as we have checked), the fraction of the mass going into the most massive object is approximately constant, and thus normalizing it by the initial mass of the stars leads to a dependence on the number of stars, as the cluster mass is fixed. As a function of stellar radius, this quantity indeed shows a power-law behavior with a slope of about 1/3. We fit the data using an implementation of the nonlinear least-squares Marquardt-Levenberg algorithm in `gnuplot` with the functions:

$$\log\left(\frac{N_{col}}{N}\right) = B\log(R_{star}) + C, \tag{2}$$

$$\log\left(\frac{M_{max}}{M_{ini}}\right) = D\log(R_{star}) + E. \tag{3}$$

The parameters of the fit are shown in Table 1. We found that E, C does not depend on N, however even if this parameters are constant, the total number of collisions N_{col} still depends on N as described in Eq. 2. We also found that D is constant but E depends on N as follows:

$$E = 0.84 \pm 0.13\log(N) - 1.96 \pm 0.39. \tag{4}$$

3.3. Description of the time evolution

For many practical applications, it will be necessary to have more information on the time evolution of the collisions. While a detailed description of every run is clearly unfeasible, our goal is to extract three main parameters that contain the most essential information. This is the time delay when most of the collisions occur, the duration of this period, as well as the total number of collisions. For this purpose, a Gaussian fit is applied to the number of collisions over time. The parameter t_{delay} describes the time when most collisions occur, $t_{duration}$ approximates the duration of the collision period. The fit is given as:

$$N_{col} = A\exp\left(-\frac{(t - t_{delay})^2}{2t_{duration}^2}\right). \tag{5}$$

The normalization A is adopted to ensure that the total number of collisions is correctly reproduced.

An example for such a fit is given in Fig. 4, showing the number of collisions in a cluster with 5000 stars and a stellar radius of 500 $R_\odot$ as a function of time. The results shown in Fig. 4 are calculated in bins of 5 crossing times as there are few collisions
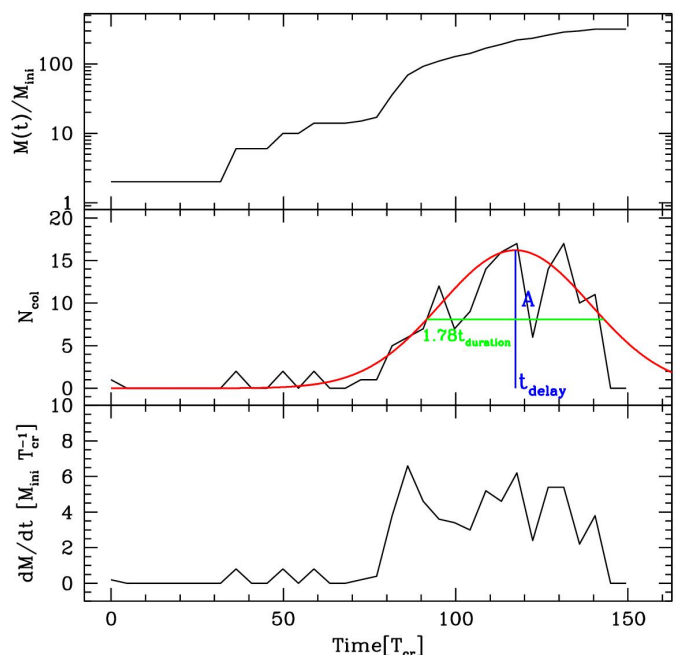
Fig. 4. Top Panel: Mass evolution of the runaway star ($M_{max}(t)/M_{ini}$) in a cluster with $N = 5000$ stars, each of them with an initial mass of $M_{star} = 2M_\odot$ and an initial radius of $R_{star} = 200\,R_\odot$. Middle panel: Number of collisions in bins of 5 crossing times (N_{col}) as function of the cluster's crossing time. The red line is the best gaussian fit. Bottom panel: Mass growth rate dM/dt in $M_{ini}\,T_{cr}^{-1}$ calculated in bins of 5 crossing times.

per crossing time and we aim for a general descriprion of the effect of collisions rather than a more individual description that depends more on statistical variatons. Nevertheless a smaller or larger binsize does not change our results as we have checked. While the time evolution of the collisions does not precisely follow a Gaussian distribution, we find that the time when most collisions occur as well as the duration of the collisions is described quite well by the Gaussian fit. For comparison, we also show the time evolution of the mass of the most massive object divided by the initial mass as a function of time. The steepest growth in mass occurs around 80 crossing times due to a collision with a 40 $M_\odot$ star formed also through stellar collisions, however, the number of collisions peaks around 120 crossing times, in agreement with a second peak in the mass enhancement, which is produced at this stage by several mergers with smaller stars. The width of the Gaussian fit matches about the time when the central object stops growing in mass. Given the overall uncertainties in the problem considered, the latter provides a reasonable description of the most relevant information.

The resulting fit parameters are given in Fig. 5 as a function of stellar radius and for different numbers of stars. The parameter A increases by a factor of 4 between 20 and 5000 $R_\odot$ for a cluster with 100 stars, while the increase is more enhanced, corresponding to about a factor of 20, for a cluster with 1000 stars. The increase of the parameter A is more moderate than naively expected from the behavior of the total fraction of collisions, which is partly due to the way how the duration of the collision period changes with the number of stars. In particular, the evolution of the $t_{duration}$ parameter as a function of stellar radius is relatively flat (slightly decreasing), and only weakly dependent on the number of stars. However, a decreasing value of t_{delay}, which quadratically enters the exponential, can overcompensate for the behavior of A. The parameter t_{delay}
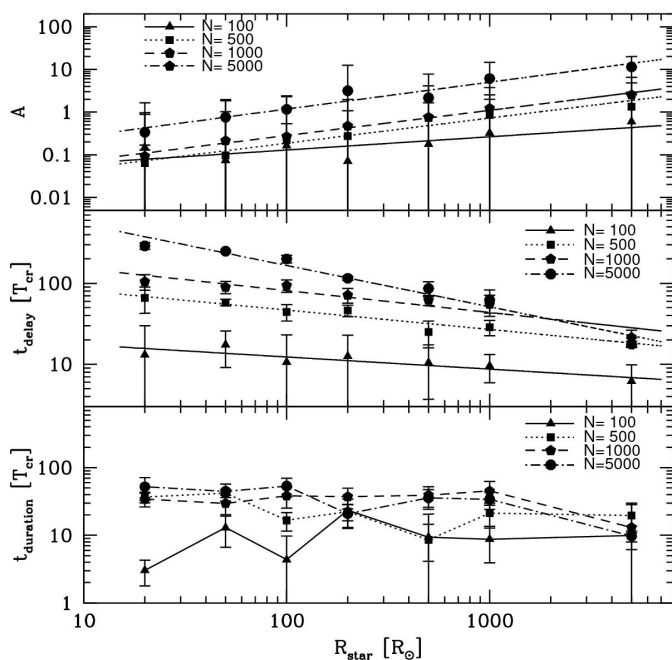
Fig. 5. Parameters of the gaussian fit A, t_{delay} and $t_{duration}$ as function of the initial stellar radii (R_{star}) and the initial number of stars N.

N	α	β	γ	δ
100	0.31±0.12	-1.51±0.29	-0.15±0.04	1.39±0.09
500	0.59±0.06	-1.91±0.16	-0.24±0.03	2.15±0.07
1000	0.63±0.07	-1.19±0.19	-0.27±0.05	2.45±0.11
5000	0.59±0.03	-1.73±0.07	-0.51±0.05	3.24±0.12

Table 2. Parameters from the fit to the functions Eq. 6 and Eq. 7 to estimate the normalization parameter A used to get the total number of collisions with the central runaway star in a cluster depending on the initial stellar radii R_{star} (Eq. 6). These parameters are also used to estimate the parameter t_{delay} which is related to the time when the rate of collisions with the central runaway star is maximum, which also depends on the initial radii R_{star} of the stars (Eq. 7).

describing the time when most of the collisions occur, on the other hand, decreases with stellar radius and increases with number of stars. This reflects in particular the increase of the relaxation time in the cluster with the number of stars, as well as the increased probability for collisions with increasing stellar radius. We fit a linear function to the quantities $\log(A)$ and $\log(t_{delay})$, with t_{delay} expressed in units of the cluster's crossing time T_{cr} depending on the logarithm of the stellar radii as follows:

$$\log(A) = \alpha \log(R_{star}) + \beta, \tag{6}$$
$$\log(t_{delay}) = \gamma \log(R_{star}) + \delta. \tag{7}$$

The parameters α, β, γ and δ are shown as function of the number of stars N in Table 2 and the fitting lines are shown in Fig. 5.

There is no clear dependence of the duration of the runaway growth on stellar radii (see bottom panel of Fig. 5). For that reason we explore the dependence of this parameter on the number of stars N. We find an exponential dependence for the duration of the runaway growth as function of the number of stars as shown in Fig. 6. The relation between $t_{duration}$ and N is

described as:

$$\log(t_{duration}) = 0.34 \pm 0.08 \log N + 0.34 \pm 0.24. \tag{8}$$

As we find no clear relation between $t_{duration}$ and R_{star} we calculate this parameter only as function of N from Eq. 8 and assume that $t_{duration}$ is constant for all stellar radii. On the other hand, we have found clear relations for $A(R_{star})$ and $t_{delay}(R_{star})$, however, these relations depend also on N (see Fig. 5). In order to get an approximate value for the number of collisions experienced by the runaway star in a star cluster consisting of N particles with a radii of R_{star} we need to take into account the dependence of A and t_{delay} on N.

Equations 6 and 7 show the dependence of A and t_{delay} on R_{star}. The slope of these relations depends on the number of stars N as described in Table 2. In order to properly account for the dependence on N when calculating the number of collisions experienced by the runaway star, we fit a line for the parameters α, β, γ and δ (related to the estimation of A and t_{delay}) as function of N. The relations we found are described as:

$$\alpha = 0.16 \pm 0.09 \log N + 0.06 \pm 0.27, \tag{9}$$
$$\beta = -0.05 \pm 0.31 \log N - 1.43 \pm 0.90, \tag{10}$$
$$\gamma = -0.21 \pm 0.05 \log N + 0.30 \pm 0.13, \tag{11}$$
$$\delta = 1.09 \pm 0.01 \log N - 0.79 \pm 0.04. \tag{12}$$

If we then combine equations 6, 7, and 9 - 12 we find A and t_{delay} as a function of N and R_{star} as described in Eq. 13 & Eq. 14:

$$\log(A) = [0.16 \log(R_{star}) - 0.05] \log(N) + 0.06 \log(R_{star}) - 1.43, \tag{13}$$
$$\log(t_{delay}) = [-0.21 \log(R_{star}) + 1.09] \log(N) + 0.30 \log(R_{star}) - 0.79. \tag{14}$$

Finally, the number of collisions experienced by the runaway star in a cluster of N stars with radii of R_{star} between times t_1 and t_2 is given by:

$$N_{col} = A \int_{t_1}^{t_2} \exp\left\{\frac{-(t - t_{delay})^2}{2t_{duration}^2}\right\} dt, \tag{15}$$

where A is calculated from Eq. 13, t_{delay} is calculated from Eq. 14 and $t_{duration}$ is calculated from Eq. 8. Time is expressed in units of the cluster's crossing time.

We solve Eq. 15 using the relations found for A, t_{delay} and $t_{duraion}$ as function of N and R_{star} for $50 \leq N \leq 10000$ and $10 \leq R_{star} \leq 2000$. We show the expected number of collisions with the central object after 1 Myr and 10 Myr in Fig. 7. If collisions need to take place within 10^6 yrs, due to the lifetime of the most massive star, the strongest collisional contributions may occur for clusters with about 1000 stars, as otherwise the characteristic timescale for the collisions to set in becomes too long. In case of stellar radii of 100 $R_{\odot}$, the enhancement by collisions corresponds to a factor of a few, which increases strongly for
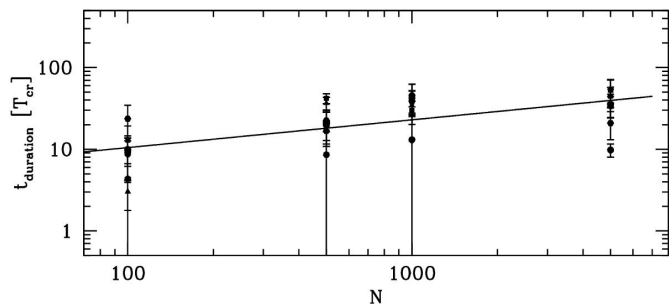
Fig. 6. Parameter t_{duration} of the gaussian fit as function of the number of stars N. We assumed that t_{duration} only depends on N and the fit is described in Eq. 8.

larger radii. In case the time available to form very massive objects is 10 million years, then the number of collisions increases as a function of N until a value of 5000 or higher, depending on the stellar radii. In such cases, relevant enhancements can be found even for stellar radii of 20 $R_\odot$, and potentially much larger for larger radii. This case is therefore the most promising case for the formation of very massive objects. It basically requires stars with less than 20 $M_\odot$, as their lifetime is then longer than 10 Myr (Schaerer 2002). Our simulations show that in stellar systems containing equal mass stars with masses M $\leq$ 20 $M_\odot$, the expected enhancement factor within 10 Myr ranges from 11-50 times the initial stellar mass M_{ini}, considering an intial stellar radius of 100 $R_\odot$ and depending on the number of stars.

In summary, we have provided a fit for N_{col} which depends on the typical duration of the collision phase t_{duration}, the delay time until collisions occur t_{delay} as well as the overall normalization A. We found that A and t_{duration} predominantly depend on the number of stars N, while t_{delay} depends both on N and R_{star}. We provide fits for the functional dependence of these parameters, and also demonstrate how the number of collisions that has occured after 1 and 10 million years depends both on N and R_{star}. We find that, as the delay time increases with N, the number of collisions within 10^6 yrs does not strongly increase with N at fixed R_{star}, but it does when considering a time of 10 Myr.

3.4. Ejections from the cluster

We also investigate the number of ejection events, which are shown in Fig. 8 both as a function of stellar radius and as a function of the number of stars. A star is considered unbound once its distance is 20 R_{vir}. For all the clusters modeled in this work, the virial radius is $R_{\mathrm{vir}} = 0.14$ pc, thus a star has escaped the cluster when it is at 2.8 pc away from the cluster center. The fraction of escaped stars seems to vary from a few up to about 20%. While there is a large scatter for a given stellar radius, the escape fraction seems independent of that quantity, while it appears to slightly decrease with the number of stars. This may particularly reflect that clusters with low numbers of stars of order 100 dissolve more easily and do not provide a well-sampled statistical distribution. We have further checked that the velocity of the escaping stars is independent of stellar radius and number of stars, and corresponds to the expected escape velocity given the mass and radius of the cluster.

While stellar ejections have not yet been systematically explored in Pop. III clusters, their potential role has been examined in different contexts. For instance, Pflamm-Altenburg & Kroupa (2010) investigated the combined effect of massive binary ejections from star clusters, including a second acceleration of a mas-
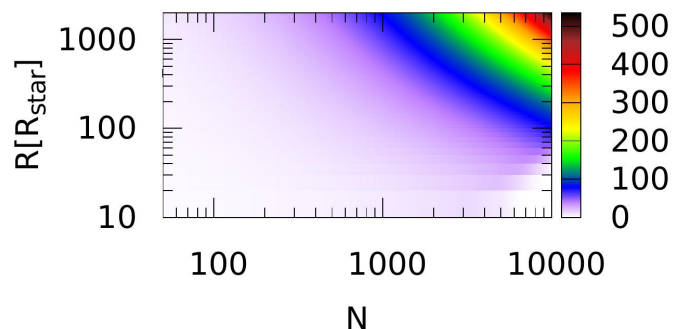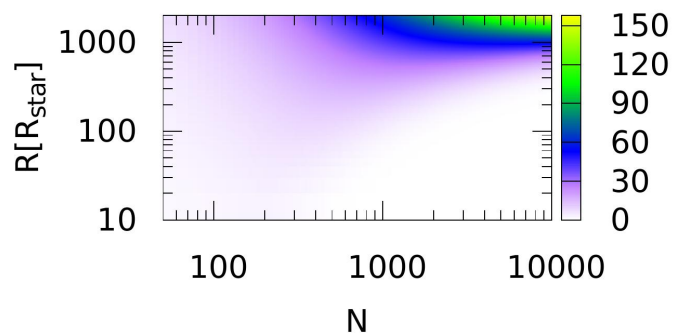

Fig. 7. Total number of collisions calculated via Eq. (15) (displayed through color) with the central object after 1 Myr (Top panel) and after 10 Myr (Bottom panel) for our cluster model depending on the number of stars and their initial radii.

sive star during a subsequent supernova. The latter may potentially help to understand the observed fraction of isolated O-star formation candidates. Oh & Kroupa (2012b) explored how the ejection of massive stars affects the relation between maximum stellar mass and cluster mass. They find that lower mass clusters do not shoot out their heaviest star, while it may occur in more massive ones. These results have been further refined by Oh et al. (2015) and Oh & Kroupa (2016), showing that star clusters of 400 $M_\odot$ are likely the dominant sources for O stars.

3.5. Uncertainties and neglected processes

In this investigation, we have not included the effect of a gaseous potential or modeled the effect of the gas in explicit terms. To zero order, if the latter is dominating the potential, it will primarily increase the velocity dispersion and thereby decrease the crossing time of the cluster, allowing for a larger number of crossing times in a given physical time. In addition, the gas may provide dynamical friction, which can potentially favor the probability of collisions. The effects of dark matter are also neglected given that at the point when the star clusters are formed, the gravitational potential is dominated by the baryons (Abel et al. 2002; Bromm & Loeb 2003).

Related to this, the accretion onto the protostars was not explicitly considered, and their masses were taken to be constant. In case that accretion contributes to the mass growth, it may again favor collisions and induce mergers of binaries that otherwise would be stable.

A further simplifying assumption employed here was that we did not consider a full initial mass function (IMF), but assumed initially uniform stellar masses. The latter has the effect to suppress three-body ejections, which may otherwise be more
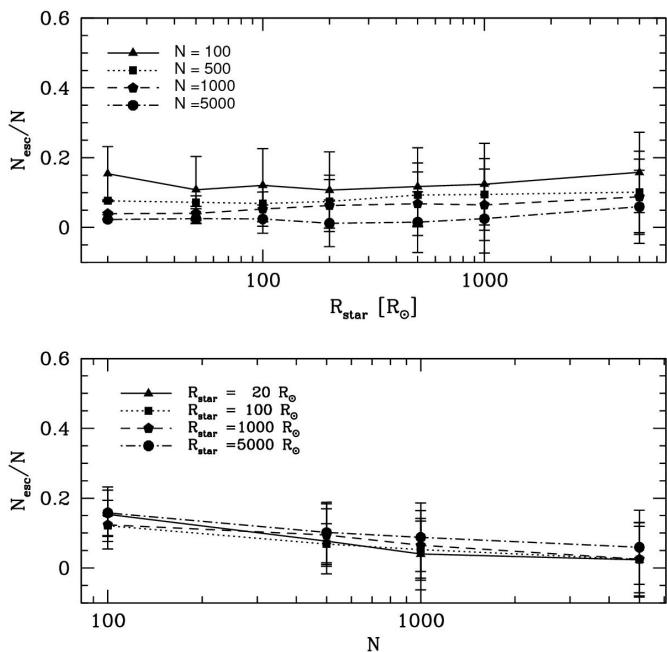
Fig. 8. Top panel: Fraction of ejections (number of ejected stars divided by the initial number of stars) as function of the initial stellar radius. Bottom panel: Fraction of ejections (number of ejected stars divided by the initial number of stars) as function of the initial number of stars.

frequent and preferably eject low-mass stars. In the presence of a logarithmically flat IMF, as it is often assumed in the context of primordial star formation (Greif et al. 2012; Hartwig et al. 2016), we do not expect this to be a major problem, though it can possible reduce the mass of the most massive object by a certain degree. We note here also that the simulations by Sakurai et al. (2017) included a full IMF, which however has not prevented the formation of a 1000 $M_\odot$ object.

In case a full IMF is considered, the next step is then clearly to take the dependence of the mass on stellar radius into account, as well as the evolution of the stellar radii over time. In this sense, our current simulations represent an effective model where an average stellar radius is adopted over the period of time considered. This effective stellar radius should correspond to the typical stellar radius at the time when the majority of collisions is expected to occur. In addition, also the "hit-and-stick" assumption employed here is valid for:

$$\sigma^2_{\text{stars}} < G \frac{M_{\text{star}}}{R_{\text{star}}}. \tag{16}$$

The velocity dispersion of the stars in all our simulations is 12.39 km s^{-1}, thus the hit-and-stick approximation should be valid for all our models except when $R_{\text{star}} = 5000\ R_\odot$. However this approximation still needs to be tested in future simulations, both to investigate how much material needs to stick for efficient growth still to occur, but also specific simulations exploring stellar collisions and merger processes would be valuable for a better understanding of possible limitations.

While clearly the processes mentioned here deserve further investigations, we will show below that the results obtained above clearly suggest the potential relevance of collisions in primordial clusters.

4. Implications for primordial clusters

In the following, we explore the implications of our results with respect to primordial star clusters. We distinguish here in particular the case of standard Pop. III clusters as expected in a typical minihalo with about $10^6\ M_\odot$, and a more massive atomic cooling halo with about $10^8\ M_\odot$.

4.1. Standard Pop. III clusters (minihalos)

For a typical Pop. III star cluster, we assume here a mass of 1000 $M_\odot$, consistent with a baryon fraction of about 10% and a star formation efficiency of order 1% in a $10^6\ M_\odot$ minihalo. We adopt here a radius of the cluster of order 0.1 pc, consistent with results from simulations and semi-analytic models (Clark et al. 2011b,a; Greif et al. 2011, 2012; Latif et al. 2013a; Latif & Schleicher 2015). We take a stellar radius of 100 $R_\odot$, which is characteristic for primordial protostars with accretion rates of the order $10^{-3}\ M_\odot$ yr^{-1} (Hosokawa et al. 2012). The crossing time of the cluster then corresponds to 0.071 Myr. The number of stars that can be expected in such a cluster is uncertain, but we adopt here an estimate of about 100.

Using the relations we found, we expect a total of about 4 collisions to occur within 1 million years. This is unchanged even if we assume a lifetime of 10 Myr, as the runaway growth occurs within 1 Myr. We expect the lifetime of a massive primordial star to be in between this range, depending on precise mass, amount of rotation and the effects the collisions may have on the stellar evolution (e.g. Maeder & Meynet 2012). We therefore find that a moderate enhancement can be achieved within a normal cluster.

We note that the values given here are the expected mean number of collisions. Individual clusters can deviate from these both towards lower and higher fractions of collisions, including potentially clusters with zero collisions. Especially for typical Pop. III clusters where the number of collisions is low, the uncertainty in the collision fraction can be expected to be comparable to the mean value.

4.2. Massive primordial clusters (atomic cooling halos)

As a next step, we address now the potential impact of collisions in a more massive atomic cooling halo. Under the right conditions, in particular if the cooling on larger scales is regulated by atomic hydrogen (e.g. Latif et al. 2014), a rather massive cluster of $10^4\ M_\odot$ can form, which will be exposed to larger accretion rates of the order $10^{-1}\ M_\odot$ yr^{-1}. We assume that the cluster consists of an initial amount of 1000 stars, and that the stellar radii are somewhat enhanced compared to the standard Pop. III cluster due to the higher accretion, with a typical value of about 300 $R_\odot$. The crossing time in the cluster is then 0.023 Myr.

Using the relations derived above, we expect about 15 collisions in 1 million years, and about 32 within 10 million years with a single runaway star. We again expect the realistic lifetime of the resulting massive star to be in between these extreme cases. In the case of an atomic cooling halo, we thus conclude that a more considerable enhancement of the mass is possible as a result of stellar collisions.

Also here, the reported values correspond to a mean, and there can be deviations to lower and higher collision fractions. We however expect the number of collisions to remain within the same order of magnitude.

5. Discussion and conclusions

In this paper, we have provided a detailed parameter study showing how the number of collisions and the growth of the mass of the most massive object depends on the properties of the stellar cluster, particularly the number of stars and the stellar radii. We have further quantified their time evolution, providing the time when most collisions occur, the duration of the peak collision period as well as the overall normalization via a Gaussian fit. We provide fits and scaling relations on the general results that we found, concerning the characteristic time delay until the maximum of collisions occurs, the duration of the period of collisions as well as the normalization that determines the number of collisions during that period. We have applied our results both to the formation of a standard Pop. III star cluster, finding a moderate enhancement of the mass of the most massive star by a factor of a few, as well as to a massive Pop. III cluster in a larger atomic cooling halo, finding a potential enhancement by a factor $15-32$.

Assuming a typical protostellar mass of $20 \, M_\odot$, this would as a result imply resulting black hole masses of up to $600 \, M_\odot$, compatible with simulation results by Katz et al. (2015) and Sakurai et al. (2017). We do however note that especially in the massive atomic cooling halos, the properties of the Pop. III clusters are not very well known, and it may be conceivable that a more massive object can form depending on mass and compactness of the clusters. Taking the results obtained here as a conservative estimate (as we neglected the gas-phase processes in this investigation), the resulting black hole masses would correspond to about $0.1 - 10\%$ of black hole masses formed via direct collapse (Koushiappas et al. 2004; Lodato & Natarajan 2007; Latif et al. 2013b; Schleicher et al. 2013; Ferrara et al. 2014).

We find both results potentially relevant. The rather modest increase of the mass of the most massive star in standard Pop. III clusters could on the one hand be relevant in case it then falls into the range of $130 - 260 \, M_\odot$ where pair-instability supernovae are expected to occur (Heger & Woosley 2002). On the other hand, as no pair-instability abundance patterns have so far been found in extremely metal poor stars (Frebel & Norris 2015), such a small factor may also explain why pair-instability supernovae did not generally occur, or have been too rare events to be found. While it is likely too early to draw definite conclusions, we expect that ongoing efforts through stellar archeology as well as the upcoming JWST[2] will shed light on this issue.

In massive Pop. III clusters, our finding that the mass of the most massive object increases can be expected to be highly relevant. This is particular because the formation of massive seeds via direct collapse still seems highly challenging, requiring both very low metallicities below $10^{-5} \, Z_\odot$ (Omukai et al. 2008; Latif et al. 2015b), as well as very strong radiation backgrounds to dissociate the molecular hydrogen (Latif et al. 2015a). Such a scenario may perhaps work as a rare event (e.g. Habouzit et al. 2016). A more recent theory suggesting the existence of mirror dark matter, that is, photons and neutrinos with the same characteristics as in the standard model of particles but interacting only via gravity, could explain the formation of 10^4-$10^5 \, M_\odot$ black holes at very high redshift, becoming SMBHs at redshift 7 wthout the need to accrete at super-Eddington rates (D'Amico et al. 2018). If collisions are taken into account, on the other hand, the formation of massive objects may become feasible under a broader range of circumstances.

However, even if fragmentation occurs, it is very likely that a relevant fraction of the mass nevertheless ends up within the most massive object, as we showed here. In these calculations,

we did not yet take into account dissipative effects such as dynamical friction, or the effects resulting from ongoing accretion onto the stars. We therefore expect that particularly within the actively accreting clusters, the number of collisions may be further enhanced, even though this could be partly balanced from the effect of having a more realistic initial mass function (IMF), that could enhance the stellar ejections. While it is clear that further investigations will be required, the present study shows clearly the prospect of forming massive objects via stellar collisions.

References

Aarseth, S. J. 2000, in The Chaotic Universe, ed. V. G. Gurzadyan & R. Ruffini, 286–287
Abel, T., Bryan, G. L., & Norman, M. L. 2002, Science, 295, 93
Ahmad, A. & Cohen, L. 1973, Journal of Computational Physics, 12, 389
Baumgardt, H. & Klessen, R. S. 2011, MNRAS, 413, 1810
Bodenheimer, P. & Sweigart, A. 1968, ApJ, 152, 515
Bonnell, I. A., Bate, M. R., & Zinnecker, H. 1998, MNRAS, 298, 93
Bovino, S., Grassi, T., Schleicher, D. R. G., & Banerjee, R. 2016, ApJ, 832, 154
Bromm, V. & Loeb, A. 2003, ApJ, 596, 34
Clark, P. C., Glover, S. C. O., Klessen, R. S., & Bromm, V. 2011a, ApJ, 727, 110
Clark, P. C., Glover, S. C. O., Smith, R. J., et al. 2011b, Science, 331, 1040
Clarke, C. J. & Bonnell, I. A. 2008, MNRAS, 388, 1171
D'Amico, G., Panci, P., Lupi, A., Bovino, S., & Silk, J. 2018, MNRAS, 473, 328
Devecchi, B., Volonteri, M., Colpi, M., & Haardt, F. 2010, MNRAS, 409, 1057
Devecchi, B., Volonteri, M., Rossi, E. M., Colpi, M., & Portegies Zwart, S. 2012, MNRAS, 421, 1465
Dopcke, G., Glover, S. C. O., Clark, P. C., & Klessen, R. S. 2011, ApJ, 729, L3
Dopcke, G., Glover, S. C. O., Clark, P. C., & Klessen, R. S. 2013, ApJ, 766, 103
Ferrara, A., Salvadori, S., Yue, B., & Schleicher, D. 2014, MNRAS, 443, 2410
Frebel, A. & Norris, J. E. 2015, ARA&A, 53, 631
Fujii, M. S. & Portegies Zwart, S. 2013, MNRAS, 430, 1018
Greif, T. H., Bromm, V., Clark, P. C., et al. 2012, MNRAS, 424, 399
Greif, T. H., Springel, V., White, S. D. M., et al. 2011, ApJ, 737, 75
Habouzit, M., Volonteri, M., Latif, M., Dubois, Y., & Peirani, S. 2016, MNRAS, 463, 529
Haemmerlé, L., Eggenberger, P., Meynet, G., Maeder, A., & Charbonnel, C. 2016, A&A, 585, A65
Haemmerlé, L., Woods, T. E., Klessen, R. S., Heger, A., & Whalen, D. J. 2017, ArXiv e-prints [arXiv:1705.09301]
Hartwig, T., Volonteri, M., Bromm, V., et al. 2016, MNRAS, 460, L74
Heger, A. & Woosley, S. E. 2002, ApJ, 567, 532
Hosokawa, T., Omukai, K., & Yorke, H. W. 2012, ApJ, 756, 93
Hosokawa, T., Yorke, H. W., Inayoshi, K., Omukai, K., & Yoshida, N. 2013, ApJ, 778, 178
Hurley, J. R., Pols, O. R., & Tout, C. A. 2000, MNRAS, 315, 543
Katz, H., Sijacki, D., & Haehnelt, M. G. 2015, MNRAS, 451, 2352
Keto, E. & Klaassen, P. 2008, ApJ, 678, L109
Klessen, R. S., Glover, S. C. O., & Clark, P. C. 2012, MNRAS, 421, 3217
Koushiappas, S. M., Bullock, J. S., & Dekel, A. 2004, MNRAS, 354, 292
Krumholz, M. R., Klein, R. I., McKee, C. F., Offner, S. S. R., & Cunningham, A. J. 2009, Science, 323, 754

---

[2] Webpage JWST: https://www.jwst.nasa.gov/

Kustaanheimo, P. & Stiefel, E. 1965, Journal für die Reine und Angewandte Mathematik, 218, 204

Larson, R. B. 1969, MNRAS, 145, 271

Latif, M. A., Bovino, S., Grassi, T., Schleicher, D. R. G., & Spaans, M. 2015a, MNRAS, 446, 3163

Latif, M. A., Omukai, K., Habouzit, M., Schleicher, D. R. G., & Volonteri, M. 2015b, MNRAS, submitted (ArXiv e-prints 1509.07034) [arXiv:1509.07034]

Latif, M. A., Omukai, K., Habouzit, M., Schleicher, D. R. G., & Volonteri, M. 2016, ApJ, 823, 40

Latif, M. A. & Schleicher, D. R. G. 2015, MNRAS, 449, 77

Latif, M. A., Schleicher, D. R. G., Bovino, S., Grassi, T., & Spaans, M. 2014, ApJ, 792, 78

Latif, M. A., Schleicher, D. R. G., Schmidt, W., & Niemeyer, J. 2013a, ApJ, 772, L3

Latif, M. A., Schleicher, D. R. G., Schmidt, W., & Niemeyer, J. C. 2013b, MNRAS, 436, 2989

Lodato, G. & Natarajan, P. 2007, MNRAS, 377, L64

Lupi, A., Colpi, M., Devecchi, B., Galanti, G., & Volonteri, M. 2014, MNRAS, 442, 3616

Maeder, A. & Meynet, G. 2012, Reviews of Modern Physics, 84, 25

Moeckel, N. & Clarke, C. J. 2011, MNRAS, 410, 2799

Oh, S. & Kroupa, P. 2012a, MNRAS, 424, 65

Oh, S. & Kroupa, P. 2012b, MNRAS, 424, 65

Oh, S. & Kroupa, P. 2016, A&A, 590, A107

Oh, S., Kroupa, P., & Pflamm-Altenburg, J. 2015, ApJ, 805, 92

Omukai, K. & Palla, F. 2001, ApJ, 561, L55

Omukai, K. & Palla, F. 2003, ApJ, 589, 677

Omukai, K., Schneider, R., & Haiman, Z. 2008, ApJ, 686, 801

Omukai, K., Tsuribe, T., Schneider, R., & Ferrara, A. 2005, ApJ, 626, 627

Palla, F. & Stahler, S. W. 1993, ApJ, 418, 414

Peters, T., Banerjee, R., Klessen, R. S., & Mac Low, M.-M. 2011, ApJ, 729, 72

Peters, T., Banerjee, R., Klessen, R. S., et al. 2010a, ApJ, 711, 1017

Peters, T., Klessen, R. S., Mac Low, M.-M., & Banerjee, R. 2010b, ApJ, 725, 134

Pflamm-Altenburg, J. & Kroupa, P. 2010, MNRAS, 404, 1564

Plummer, H. C. 1911, MNRAS, 71, 460

Rees, M. J. 1984, ARA&A, 22, 471

Sakurai, Y., Yoshida, N., Fujii, M. S., & Hirano, S. 2017, ArXiv e-prints [arXiv:1704.06130]

Schaerer, D. 2002, A&A, 382, 28

Schleicher, D. R. G., Palla, F., Ferrara, A., Galli, D., & Latif, M. 2013, A&A, 558, A59

Schneider, R., Ferrara, A., Salvaterra, R., Omukai, K., & Bromm, V. 2003, Nature, 422, 869

Schneider, R., Omukai, K., Inoue, A. K., & Ferrara, A. 2006, MNRAS, 369, 1437

Schneider, R., Omukai, K., Limongi, M., et al. 2012, MNRAS, 423, L60

Shu, F. H. 1977, ApJ, 214, 488

Smith, R. J., Glover, S. C. O., Clark, P. C., Greif, T., & Klessen, R. S. 2011, MNRAS, 414, 3633

Smith, R. J., Hosokawa, T., Omukai, K., Glover, S. C. O., & Klessen, R. S. 2012, MNRAS, 424, 457

Stahler, S. W., Palla, F., & Salpeter, E. E. 1986, ApJ, 302, 590

Woods, T. E., Heger, A., Whalen, D. J., Haemmerlé, L., & Klessen, R. S. 2017, ApJ, 842, L6

Yorke, H. W. & Sonnhalter, C. 2002, ApJ, 569, 846